Neurobiology of Pain 14 (2023) 100142

Contents lists available at ScienceDirect

Neurobiology of Pain

journal homepage: www.sciencedirect.com/journal/neurobiology-of-pain

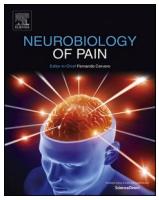

circRNA landscape in dorsal root ganglia from mice with collagen antibody-induced arthritis

Zerina Kurtović [a,b], Katalin Sandor [a], Freija ter Heegde [a], Resti Rudjito [a], Camilla I. Svensson [a,2,*], Vinko Palada [a,2,1]

[a] Department of Physiology and Pharmacology and Center for Molecular Medicine, Karolinska Institutet, Solna, Sweden
[b] Kancera AB, Karolinska Institutet Science Park, Solna, Sweden

ARTICLE INFO

Keywords:
Circular RNA
CAIA
Dorsal root ganglia
Chronic pain
Arthritis

ABSTRACT

Circular RNAs are a novel class of RNA molecules that are covalently closed into a ring structure. They are an epigenetic regulatory mechanism, and their best-studied function is regulation of microRNA activity. As such circular RNAs may be involved in the switch from acute to chronic pain. They have previously been studied in the context of neuropathic pain models, but their importance in inflammation-induced chronic pain models is unexplored. Microarray analysis of dorsal root ganglia collected in the late phase of collagen antibody-induced arthritis (day 59) were used to elucidate the relevance of circular RNAs in the mechanical hypersensitivity caused by this model. 120 circular RNA genes were found to be significantly differentially regulated in female BALB/c mice with collagen antibody-induced arthritis. Six genes were chosen for RT-qPCR analysis in the late (day 54–60) as well as the inflammatory (day 11–12) phase of this model. This validated an increase in *circNufip1* expression in the late phase of collagen antibody-induced arthritis. Additionally, it was found that *circVps13* and *circMicall1* are upregulated in the inflammatory phase. Interestingly, no changes were found in dorsal root ganglia from mice injected with Freund's Complete Adjuvant (day 3) nor mice with spared nerve injury (day 20), despite their similarities to inflammatory and late phase collagen antibody-induced arthritis, respectively. This study provides evidence that mild circular RNA changes occur in dorsal root ganglia of mice with collagen antibody-induced arthritis that are, bioinformatically, predicated to be involved in processes relevant to sensitization.

Introduction

The underlying mechanisms of chronic pain are complex and involve a combination of biological, psychological, and social factors (Cohen et al., 2021). At the molecular level, chronic pain is characterized by changes in a large number of genes in the peripheral and central nervous system. Over the past decade, increasing number of studies have shown that epigenetic modifications play a crucial role in regulating gene expression associated with chronic pain (Descalzi, 2015; Polli et al., 2020). There are three primary epigenetic mechanisms: DNA methylation, histone modification, and regulation mediated by non-coding RNAs (ncRNAs). The most extensively studied ncRNAs include microRNA (miRNA), long non-coding RNA (lncRNA), and circular RNA (circRNA). While there is extensive data on the role of miRNA in long-lasting nociception, circRNAs have just emerged as players in the development of chronic pain.

CircRNA is a unique type of non-coding RNA with a covalently closed ring structure that is formed from RNA via a process called back-splicing. Adding *circ* to the name of the linear gene found in the locus from which the circRNA is transcribed is the most common way to name circRNAs, although calls have been made for more precise nomenclature (Chen, 2023). The best described function of circRNAs is acting as sponges for miRNAs and in that way regulating gene expression (Zhou, 2020; Song et al., 2020). CircRNAs may also serve as scaffold for protein complexes and regulate the activity of proteins as well as the translation and stability of mRNA levels (Kristensen, 2019). CircRNAs are widely expressed in mammals and found in a wide range of cells with a tissue specific pattern (Patop et al., 2019). They are abundant in the brain and

* Corresponding author at: Karolinska Institutet, Biomedicum B5, 171 77 Stockholm, Sweden.
E-mail address: camilla.svensson@ki.se (C.I. Svensson).
[1] Current affiliation: Department of Physiology and SleepWell Research Programme, Faculty of Medicine, University of Helsinki, Helsinki, Finland.
[2] These authors share senior authorship.

https://doi.org/10.1016/j.ynpai.2023.100142
Received 18 July 2023; Received in revised form 24 August 2023; Accepted 28 August 2023
Available online 3 September 2023

neuronal cell lines (Patop et al., 2019; Rybak-Wolf, 2015) and a growing body of evidence indicates that circRNAs are involved in various neurological disorders, including pain (Cao, 2017). Differential expression of circRNAs has been reported in several models of neuropathic pain. In rats subjected to the chronic constriction injury model, differential expression of 469 circRNA genes was reported in the ipsilateral lumbar spinal dorsal horn (Cao, 2017) and in following spared nerve injury in rats, 188 circRNA genes were altered in rat lumbar spinal dorsal horn (Zhou et al., 2017). Transection of the sciatic nerve in mouse led to differential expression of about 500 circRNAs both proximally and distally to the transection (Sohn and Park, 2020). Diabetic peripheral neuropathy was associated with differential expression of 15 circRNAs (Zhang et al., 2020) and paclitaxel-induced neuropathy with 16 differentially expressed circRNAs (Mao, 2022) in dorsal root ganglia (DRG). Furthermore, crush (Mao, 2019) and chronic constriction (Xiong, 2022) of the sciatic nerve in rat lead to differential expression of 1060 and 374 circRNAs in DRG, respectively. Analyses of differential expression of circRNAs in rat DRG after injury to the dorsal root or peripheral nerve have been compared (Cao et al., 2022), showing 33 versus 55 differentially expressed circRNAs after injury with only partial overlap in terms of circRNA profiles and signaling pathways triggered by the different injuries (Cao et al., 2022). These studies together indicate that circRNAs are important factors during neuropathic pain development at multiple anatomical sites of pain signaling.

While mounting data indicate that the circRNA expression can be altered at various levels along the pain-axis upon peripheral nerve injury, less is known about the regulation of circRNA expression associated with inflammation-induced persistent pain. However, a number of circRNAs have been implicated in the pathogenesis of rheumatoid arthritis (RA), a chronic autoimmune disease characterized by joint inflammation and joint pain and shown to be differentially expressed in peripheral blood mononuclear cells (PBMCs) and synovial fluid from RA patients compared to healthy controls (Wang, 2020; Yang et al., 2020). Furthermore, knockdown of specific circRNA genes in mice with collagen-induced arthritis was shown to reduce joint inflammation, though the impact on pain-related behaviors was not examined (Yang et al., 2020). While it is well established that inflammatory processes in the joint contribute to pain in RA, the observation that pain can persist despite adequate control of the inflammatory process indicates that multiple mechanisms are at play (McWilliams and Walsh, 2017). The notion that different mechanisms contribute to pain during and between disease flares is supported by findings in antibody-induced arthritis animal models of RA. These reports indicate that the pronociceptive mechanisms at least partly differ between the early (inflammatory) and late (post-inflammatory) phases of the models (Christianson et al., 2010; Christianson et al., 2011; Bas, 2012; Agalave et al., 2014; Rudjito, et al., 2021; Allen et al., 2020; Su, 2015; Su, 2022). In this study we used the collagen antibody-induced arthritis (CAIA) model, which causes joint inflammation that resolves 3–4 weeks after injection of anti-collagen type II antibodies (Bas, 2012). Mice subjected to CAIA develop mechanical hypersensitivity which, in contrast to the transient inflammation, is persistent and lasts for weeks after the visual signs of inflammation have resolved (Bas, 2012). The aims of this study was to i) examine the circRNA profile in DRG from mice subjected to antibody-induced arthritis and ii) explore the potential contribution of circRNAs in the transition from inflammatory-driven pain to non-resolving persistent pain by comparing regulation of specific circRNAs in DRG between the inflammatory and late phase of the CAIA model and models of acute joint inflammation and nerve injury.

Methods

Animal models

All experiments were carried out in accordance with protocols approved by the local ethics committee for animal experiments in Sweden (Stockholms Norra Djurförsöksetiska Nämnd, number of ethical permits: N183/15, 12127–2020 and 9013–2020). Adult female BALB/c mice (12 weeks old) were housed in standard conditions on a 12-hour light/dark cycle. Food and water were available ad libitum. As the incidence and severity of CAIA in male BALB/c mice at the animal facility used during this study is low and arthritis is more common in women than in men, only female mice were used in this study.

Collagen antibody-induced arthritis (CAIA)

CAIA was induced by intravenous (i.v.) injection of 1.5 mg anti-collagen type II (CII) antibody cocktail (Chondrex, Redmond, WA) on day 0, followed by intraperitoneal (i.p) injection of 25 μg lipopolysaccharide (LPS, Chondrex) on day 3 or 5. The control group received 150 μl of saline i.v. on day 0 and 100 μl saline i.p. on day 3 or 5. Days 6–42 are considered the inflammatory phase and timepoints after day 52 are considered the late phase (starting 10 days after arthritis scores < 2).

Complete Freund's Adjuvant (CFA)-induced monoarthritis

CFA-induced monoarthritis was induced by an intra-articular (i.a.) injection of 5 μl CFA (10 mg/ml, Chondrex) into one ankle joint using a 29-G needle to mice anesthetized with isoflurane (induction, 5%; maintenance, 2.5%). Control mice received an i.a. injection of 5 μl PBS into the ankle joint.

Spared nerve injury (SNI) model

Mice were given a subcutaneous injection of Buprenorphine and anesthetized with isoflurane and the ipsilateral thigh shaved and cleaned with 2% chlorhexidine or 70% ethanol. A skin and muscle incision was made in the thigh to expose the sciatic nerve. A tight ligature using a 6–0 silk suture was placed around the tibial and common peroneal branches, after which the nerves distal to the ligatures were transected. The third branch, the sural nerve, was left intact and stretch or contact carefully avoided (Rudjito, et al., 2021). Sham surgeries were done identically to the SNI surgery; however, no portion of the sciatic nerve was ligated or transected. The skin was closed using surgical sutures and mice were then given a subcutaneous injection of Buprenorphine, which was repeated with 8–12 h intervals until the end of day 3.

Behavioral test and arthritis scoring

Paw withdrawal thresholds were measured using von Frey filaments. Mice were habituated to the testing cages, individual compartments on top of a wire-mesh surface (Ugo Basile), before baseline recordings. On test days, mice were first habituated to the test environment for 1 h before testing. Withdrawal thresholds were assessed by application of OptiHair filaments (Marstock OptiHair) of increasing stiffness (0.5, 1, 2, 4, 8, 16, and 32 mN, corresponding to 0.051, 0.102, 0.204, 0.408, 0.815, 1.63, and 3.26 g, respectively) to the plantar surface of the paw. A brisk withdrawal of the paw from the filament within 2–3 s was noted as a positive response. The 50% probability withdrawal threshold (force of the von Frey filament to which an animal reacts to 50% of the presentations) was calculated using the up–down method (Chaplan et al.,1994). Mechanical sensitivity was measured and averaged values for both hind paws. The mice were assigned to the different groups by stratified randomization based on their withdrawal thresholds (average of 3–5 baselines) in order to avoid baseline values to be a confounding factor. The experimenter was blinded during the study. The level of inflammation was assessed in all four limbs based on a scoring system. An inflamed toe was noted as one point; inflamed paws and the ankle joints were scored 2.5 or 5 depending on the level of inflammation as previously described (Bas et al., 2012).

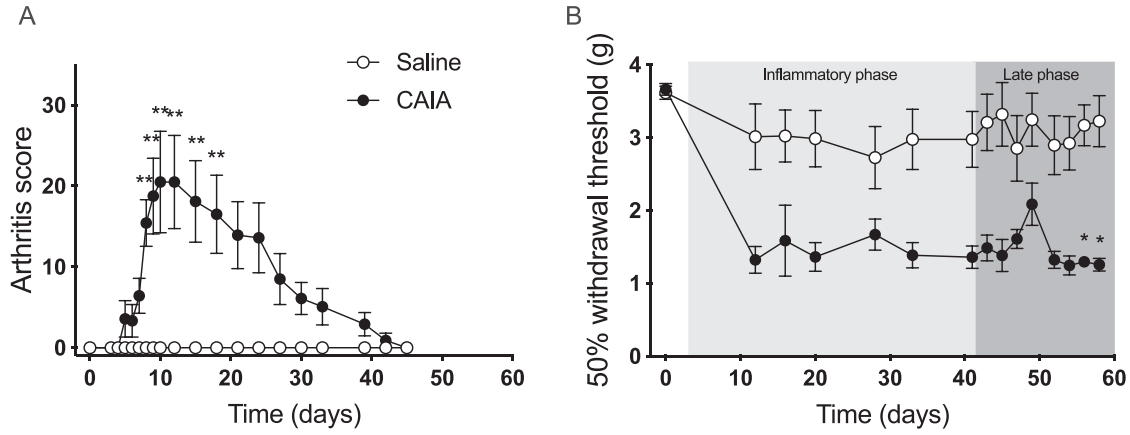

Fig. 1. Time course of disease severity and pain-like behavior in the CAIA model. (A) Mice were evaluated by visual inspection for disease severity, assessed as the arthritis score (scale of 0–60, range 0–15/paw). Arthritis scores were compared using multiple Mann-Whitney tests, followed by two-stage step-up correction for multiple comparison (Benjamini, Krieger, and Yekutieli). The error bars represent the SEM. (B) Withdrawal thresholds in the hind paws were assessed by Von Frey filaments prior to injection and throughout the experimental period. Two-way ANOVA was preformed followed by Šídák's multiple comparisons test for correction of multiple comparison. Data are presented as mean +/-SEM, n = 6 mice/group. Tissues from these animals were included in the qPCR analysis (n = 6) described in Fig. 4.

RNA isolation and quality control

Mice were euthanized and decapitated under isofluorane anesthesia day 11–12 (inflammatory phase) or 54/60 (late phase) after induction of CAIA, day 3 after injection CFA and day 20 after SNI surgery. L3-L5 DRG were dissected, fresh frozen and stored at − 70 °C until analysis. For RNA extraction, the frozen DRG samples were placed to tubes with glass beads and lysed with the use of a Precellys 24 tissue homogenizor (Bertin Instruments) in TRIzol reagent (Thermo Fisher) according to the manufacturer's protocol. RNA samples were treated with DNAse (Qiagen) and the RNA amount of each sample was determined by OD260 using a NanoDrop ND-1000 instrument (NanoDrop Thermo). The Agilent Bioanalyzer 2100 (Agilent technologies, CA, USA) instrument was used to inspect RNA integrity number (RIN).

Microarray and data analysis

The sample preparation and microarray hybridization were performed based on the Arraystar's standard protocols (Arraystar Inc, Rockville, MD, USA)0.31 Briefly, total RNAs were digested with Rnase R (Epicentre, Inc., Madison, WI, USA) to remove linear RNAs and enrich circRNAs. Then, the enriched circRNAs were amplified and transcribed into fluorescent circRNA utilizing a random priming method (Arraystar Super RNA Labeling Kit; Arraystar). The labeled circRNAs were purified by RNeasy Mini Kit (Qiagen) and 1 μg of each labeled circRNA was fragmented by adding 5 μl 10 × Blocking Agent and 1 μl of 25 × Fragmentation Buffer, then heated the mixture at 60 °C for 30 min. Finally, 25 μl 2 × Hybridization buffer was added to dilute the labeled cRNA and 50 μl of hybridization solution was dispensed into the gasket slide and assembled to the Arraystar Mouse circRNA Array V2 (8x15K, Arraystar Inc, 15 236 circRNAs). The slides were incubated for 17 h at 65 °C in an Agilent Hybridization Oven and after washing, the arrays were scanned by the Agilent Scanner G2505C (Agilent Technologies, Santa Clara, CA, USA). Agilent Feature Extraction software (version 11.0.1.1) was used to analyze acquired array images. Quantile normalization and subsequent data processing were performed using the R software limma package. Differentially expressed circRNAs with statistical significance between two groups were identified through volcano plot filtering. Differentially expressed circRNAs between two samples were identified through fold change filtering. Hierarchical clustering was performed to show the distinguishable circRNAs expression pattern among samples.

Real-time quantitative PCR (qPCR) analysis

Purified total RNA (250 ng) was reversed transcribed to cDNA using the High-Capacity cDNA Reverse Transcription Kit with RNase Inhibitor (ThermoFischer) according to manufacturer's protocol. The qPCR reactions were performed in duplicate for each sample using the iTaq Universal SYBR Green Supermix (BioRad) in a Bio-Rad CFX Maestro 1.1 (BioRad) according to the manufacturer's instructions. A total of six differentially expressed circRNAs from the microarray dataset were additionally investigated by qPCR using divergent primers which were designed to overlap the back-spliced junctions of circRNAs (the forward primer being located downstream of the reverse primer when they are aligned to genomic sequence). Three circRNAs with the largest fold change (*circNufip1*, *circVps13c*, *circMicall1)* and three circRNAs from loci that have previously been reported to have roles in pain regulation (*circCpa6*, *circGrm1*, *circTrpm3*[38-43]) were selected. The sequences of divergent primers are listed in Table S1. The housekeeping gene *Hprt* was used as a reference control. Primer sequences are listed in Table S1. The 2-ΔΔCt method was used to calculate the relative levels of selected circRNAs. Data is expressed as fold change from control.

Bioinformatical analysis

Interactions between circRNAs and miRNAs were predicated with Arraystar's home-made miRNA target prediction software based on TargetScan and miRanda. These were uploaded into miRWalk and the resulting list of target genes were used to perform Reactome analysis in miRWalk (Dweep et al., 2011). The results shown have been filtered for $p < 0.05$.

Statistical analysis

Data is presented as the mean and the error bars are the standard error of mean (SEM). For comparison of pain-like behavior, a two-way analysis of variance (ANOVA) with Šídák's or Tukey multiple comparisons test for repeated measures was used, while for comparison of clinical score the Mann-Whitney test, followed by two-stage step-up correction for multiple comparison Benjamini, Krieger, and Yekutieli. Student's *t*-test was used for data analysis apart from the validation of the microarray results with qPCR. The Rout test (Q = 1%) was used to identify outliers. For this data, a one-tailed test was used as the direction of change was expected. The remaining t-tests were two-tailed.

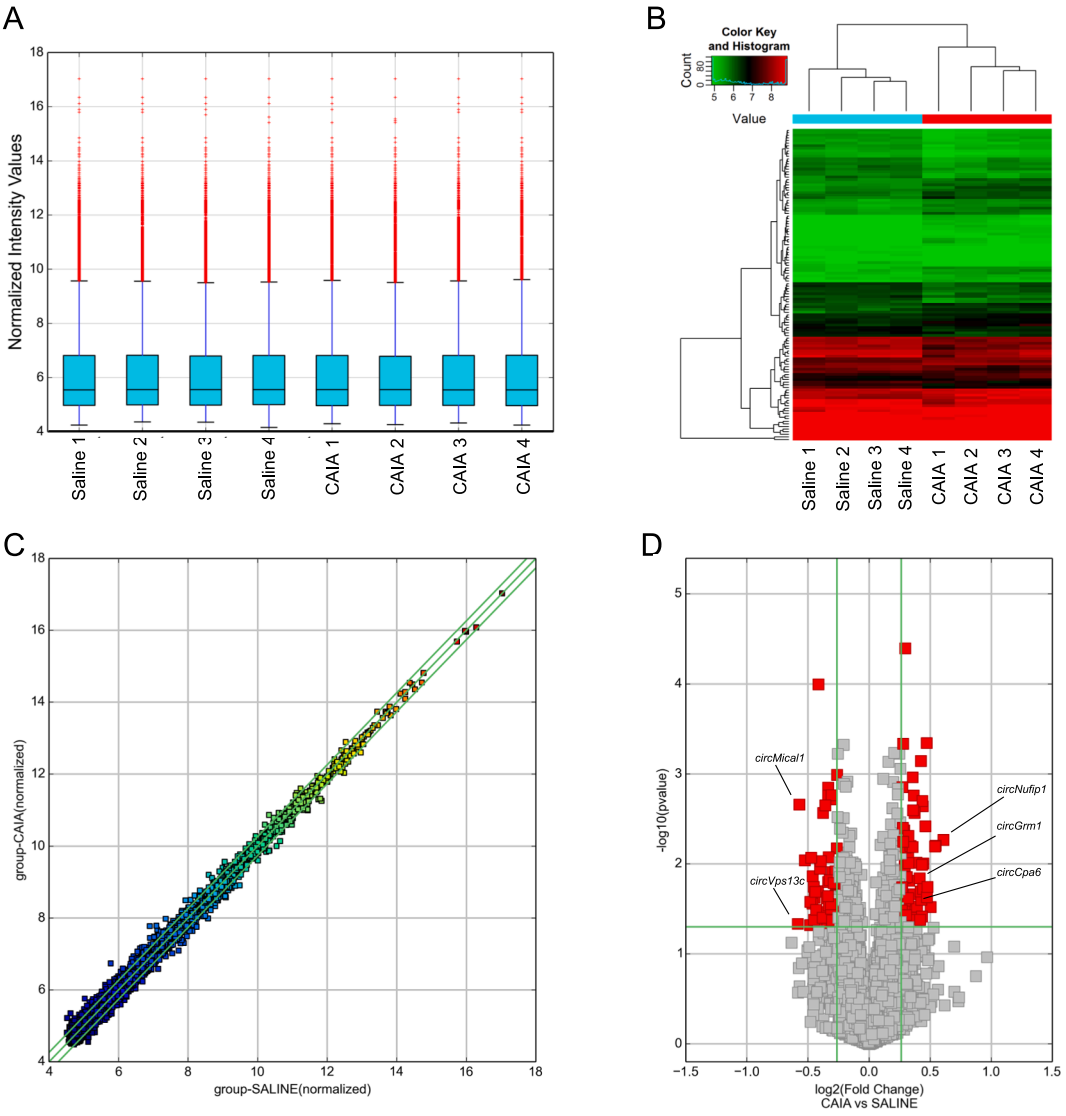

Fig. 2. Mild differences in expression of circRNAs in DRG in the late phase of the CAIA model. (A) All samples were normalized. (B) Heatmap and hierarchy tree showing that mild changes in overall expression are consistently present between CAIA and saline samples but as is also seen from the dotplot in (C), no single gene shows drastic differences in expression. (D) Volcano plot of -$\log_{10}$(p-value) versus $\log_2$(Fold change) shows that even though not numerous, some circRNAs are differentially regulated between CAIA and saline control and the differences are statistically significant (red). (For interpretation of the references to colour in this figure legend, the reader is referred to the web version of this article.)

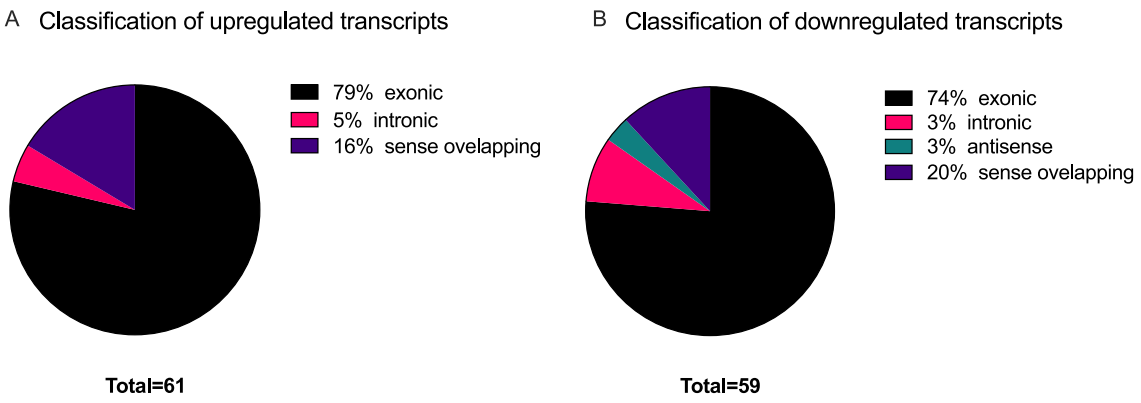

Figure 3. Description of the classification of transcripts that are included in table S2 (A) and S3 (B).

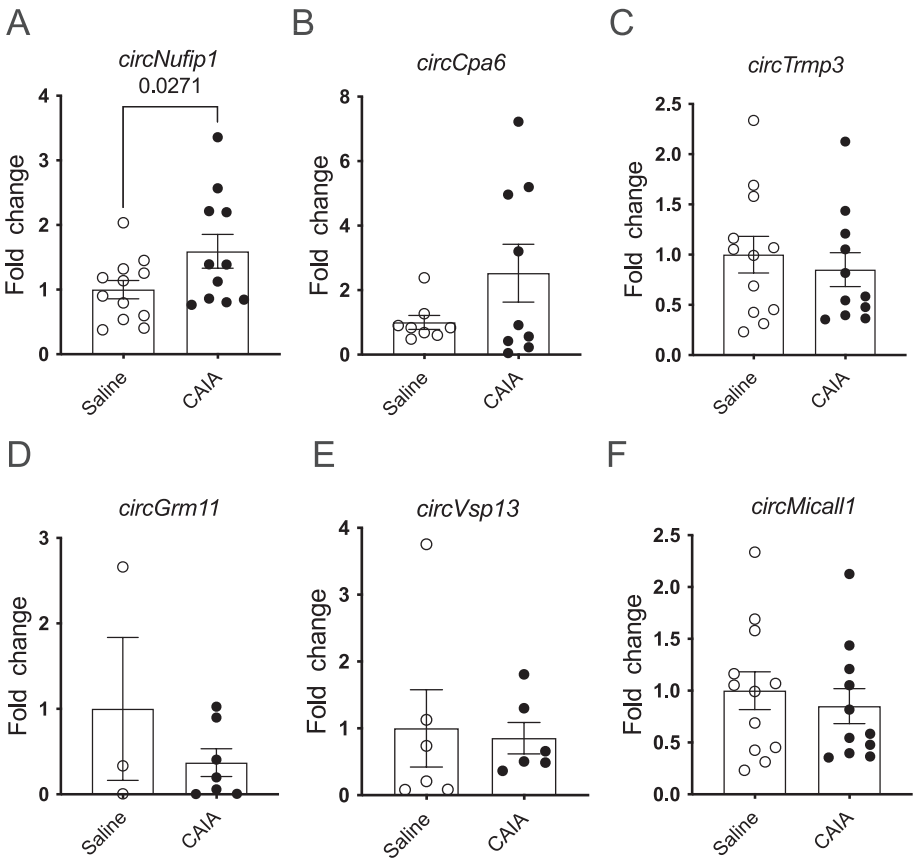

Fig. 4. Expression of selected genes measured with qPCR. (A-F) Gene expression of 6 selected circRNA assessed in DRG from the late phase of the CAIA model (n = 12, the missing data points indicate that the gene was not detected in the sample). One-tailed *t* test was performed. Data are presented as individual values and bar with error bar represent mean +/-SEM.

GraphPad Prism 8 and was used for statistical analysis. $P < 0.05$ was considered statistically significant.

Results

Development of transient joint inflammation and long-lasting mechanical hypersensitivity in mice after induction of CAIA

Female Balb/c mice with CAIA developed joint inflammation in both front and hind legs, which peaked around day 10 after injection of anti-CII antibodies (Fig. 1A) and then slowly resolved. Withdrawal thresholds assessed by Von Frey filaments showed that mice subjected to CAIA develop mechanical hypersensitivity that was readily detectable during peak inflammation, but in contrast to the resolving joint inflammation, did not resolve and persisted throughout the experimental period (Fig. 1B). In this study days 6–42 were considered the inflammatory phase time points and days 52–59 the late phase.

Microarray analysis of circRNA in dorsal root ganglia from the late phase of the CAIA model

DRG (L3-L5) were collected 59 days after injection of anti-CII antibodies or saline and processed for circRNA microarray analysis. In total 8676 circRNA genes were identified and the intensity of all the samples after normalization are displayed by box plot (Fig. 2A). Differentially expressed circRNAs between the saline and CAIA groups were determined based on fold change filtering (Table S2 and S3). By applying a fold change (FC) > 1.20 and $p < 0.05$, 61 circRNA were identified upregulated and 59 downregulated. Hierarchical clustering was performed to visualize the differential circRNAs (Fig. 2B). The differentially expressed genes are listed in Table S2 (upregulated) and Table S3 (downregulated). In terms of genomic element, the majority of both upregulated and downregulated transcripts mapped to exonic parts of the mouse genome (Fig. 3A-B); upregulated circRNAs included 48 exonic, 3 intronic, 0 intergenic, 0 antisense and 10 sense overlapping (Fig. 3A), while the downregulated circRNAs included 45 exonic, 5 intronic, 0 intergenic, 2 antisense and 7 sense overlapping (Fig. 3B). In summary, the microarray data shows that CAIA induces subtle differences in circRNA expression compared to control mice.

qRT-PCR verification of differentially expressed circRNAs from microarray

Out of 6 differentially expressed circRNAs in microarray that were selected for validation by quantitative real-time-PCR, four were upregulated in CAIA versus saline controls (*circCpa6, circNufip1, circGrm1, circTrpm3*) and 2 were downregulated (*circMicall1* and *circVps13*). The expression of selected circRNAs in late phase CAIA was examined by qPCR in a total of 12 CAIA and 12 control L3-L5 DRG samples. Similarly, to microarray, DRG expression of *circNufip1* was increased 1.6 folds in late CAIA (one-tailed *t*-test, $p = 0.027$), while no difference was observed between the late CAIA and control groups for *circCpa6, circGrm1, circTrpm3, circMicall1 and circVps13* (Fig. 4 A-F).

DRG expression of selected circRNA from CAIA late phase is not altered in SNI model of neuropathic pain

Changes in DRG mRNA levels and protein expression in the late phase of the CAIA model show some similarities with changes reported in DRG from mice subjected to experimental models of neuropathic pain

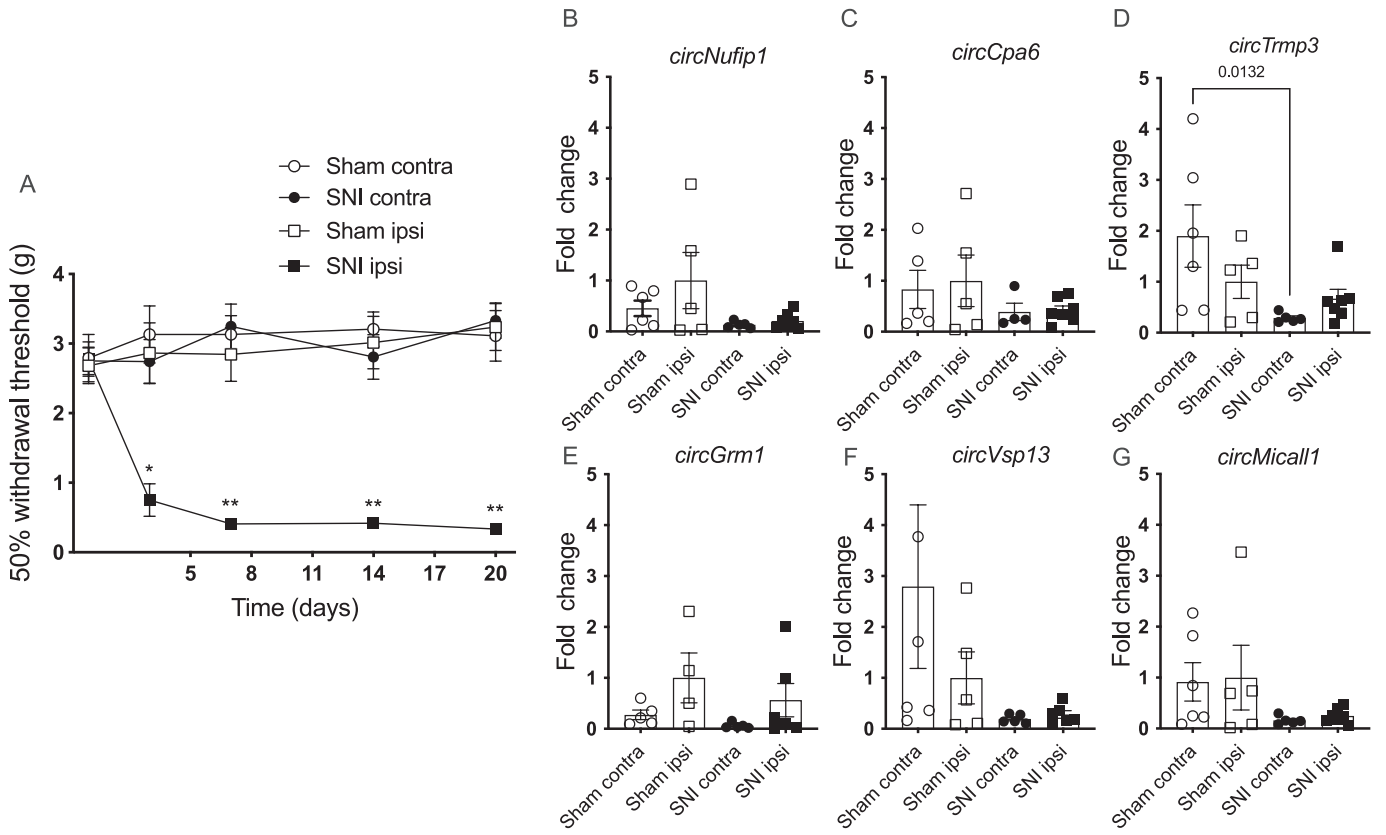

Fig. 5. Mechanical hypersensitivity and expression of selected circRNA targets in DRG after SNI surgery. (A) Withdrawal thresholds assessed by Von Frey filament. Two-way ANOVA was performed followed by Tukey multiple comparisons test and data are presented as mean +/-SEM, n = 6–7 mice/group. (B-G) Expression of six selected genes measured with qPCR in DRG collected 20 days after SNI or sham surgery (n = 6–7, the missing data points indicate that the gene was not detected in the sample). Unpaired *t* test was preformed, error bars represent the SEM.

(Zhang et al., 2020). To investigate if changes in the six circRNA transcripts selected from the CAIA microarray were more pronounced after nerve injury, we collected L3-5 from mice subjected to SNI. Female BALB/c mice underwent either sham surgery or sciatic nerve injury and the SNI mice showed long-lasting mechanical hypersensitivity on the ipsilateral hindpaw (Fig. 5A) as compared to the sham ipsilateral hindpaw. The withdrawal thresholds of SNI contralateral and sham contralateral paws did not differ from baseline values at any time point of testing. Three weeks after the surgery (day 20), L3-L5 DRG were collected from the contralateral and ipsilateral sides and used for qPCR analysis. We did not find any statistically significant differences in levels of the six circRNAs when comparing ipsilateral to contralateral DRG from mice with SNI or ipsilateral SNI versus ipsilateral sham DRG (Fig. 5 B-G).

Several of the selected circRNAs are upregulated in DRG in the inflammatory phase of CAIA but not in the CFA model of joint inflammation

As we did not see any difference in the six circRNAs in DRG from mice with SNI, we next investigated if the indication of changes observed in the late phase of the CAIA model were associated with the inflammatory aspects of the model. Therefore, we collected DRG from the inflammatory phase of the CAIA model as well as from mice subjected to CFA-induced monoarthritis. The course of joint inflammation and mechanical hypersensitivity in the CAIA model prior to termination and collection of DRG day 12 (Fig. 6A-B) were similar to the CAIA late phase experiment (Fig. 1A-b). Unlike the late phase, *circNufip1* in DRG is not differentially expressed in the inflammatory phase when comparing levels in CAIA to control mice (Fig. 6C). Interestingly, the two circRNA genes that were downregulated in the late phase of the CAIA model in the array dataset; *circVsp13* and *circMicall1*, were both upregulated in the inflammatory phase (Fig. 6G-H). The *circCpa6*, *circTrmp3* and *circGrm11* were not significantly changed in DRG from CAIA mice compared to controls in the inflammatory phase (Fig. 6C-F). CFA-induced monoarthritis results in a rapidly developing joint inflammation and mechanical hypersensitivity on the ipsilateral side detectable already on day 1 (Fig. 7A). DRG were collected 3 days after CFA-injection and circRNA levels compared between the ipsilateral and contralateral side. None of the examined circRNAs were differentially expressed in the CFA model comparing ipsi to contralateral DRG (Fig. 7B-C).

Bioinformatical investigation of potential functions of circNufip1, circVsp13 and circMicall1

The functional relevance of an upregulation of *circNufip1* was explored bioinformatically using the online tool *miRWalk* (Table 1). The miRNA binding sites were predicted by the circRNA array analysis and were used to run the miRWalk analysis. The terms included in Table 1 had a p-value < 0.05. Notably, the reactome results predicted that *circNufip1* could contribute to development of long-term potentiation and chronic pain via unblocking of NMDA receptors, glutamate binding and activation.

We also performed the miRWalk bioinformatical analysis on the miRNAs predicted to bind *circVsp13c* and *circMicall1*. Notably, the reactome terms resulting from the analysis, listed in Table 2 and 3, include immune-related processes which likely reflect the fact that the DRG were analyzed at the timepoint of peak joint inflammation.

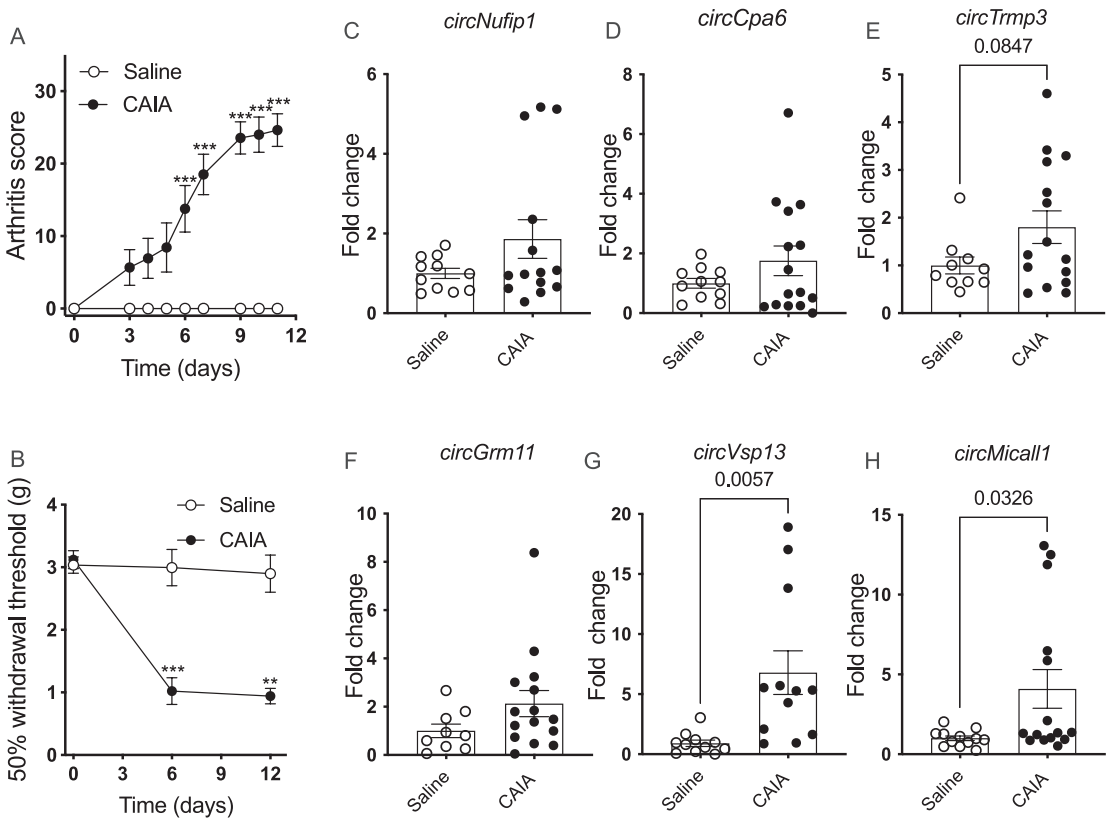

Fig. 6. Arthritis scores, mechanical hypersensitivity and expression of selected circRNA targets in DRG form the inflammatory phase of CAIA (day 10–12). (A) Arthritis scores of the animals included in the qPCR analysis. Multiple Mann-Whitney tests, followed by two-stage step-up correction for multiple comparison (Benjamini, Krieger, and Yekutieli) were used to compare the arthritis scores and the error bars represent the SEM. (B) Withdrawal thresholds assessed by Von Frey filaments. Two-way ANOVA was preformed followed by Šídák's multiple comparisons test. Data in A and B are presented as mean +/-SEM, n = 10 mice/group. (C-H) Expression of the selected genes measured with qPCR in samples from animals sacrificed in the inflammatory phase of CAIA (n = 12 for saline and n = 15 for CAIA, the missing data points indicate that the gene was not detected in the sample). Unpaired *t* test was performed, error bars represent the SEM.

Discussion

To our knowledge, this is the first study aiming to profile the circRNA transcriptome in DRG from the CAIA mouse model of RA. In addition, we assessed the change in expression profiles of selected circRNAs in the inflammatory phase of CAIA, when joint inflammation is present and in the late phase, when inflammation has resolved but persistent mechanical hypersensitivity resembling neuropathic pain-like conditions persist. Our circRNA microarray data revealed 61 upregulated and 59 downregulated circRNAs in DRG from the late phase of CAIA.

Interestingly, when comparing the expression of selected circRNAs from the microarray between inflammatory and late phases of CAIA using qPCR, we could not confirm the change of *circVsp13* and *circMicall1* expression in the late phase but found that *circVsp13* and *circMicall1* were upregulated in the inflammatory phase of the model. In contrast, *circNufip1* levels were reduced in the late phase assessed both by microarray and qPCR but was not different from control in the inflammatory phase of the model. Furthermore, *circNufip1*, *circVsp13 and circMicall1* were not altered in DRG from the CFA and SNI mouse models, indicating that the observed changes in circRNA expression are specific to CAIA.

In recent years, circRNAs have emerged as a new class of non-coding RNAs that are involved in regulation of painful conditions. While the connection between circRNAs and regulation of neuropathic pain is well established (Zheng et al., 2022), the potential role of circRNAs in inflammatory pain conditions such as RA remains largely unexplored. One previous study reported that inflammatory hypersensitivity can be attenuated by silencing *circRNA-Filip1l* (filamin A interacting protein 1-like) in the spinal cord of mice with CFA-induced inflammation (Pan, 2019). Based on our microarray analysis, *circRNA-Filip1l* was not differentially expressed in the DRG from the late phase of the CAIA model. In fact, our top 3 differentially expressed circRNAs on the microarray, *circNufip1*, *circVsp13* and *circMicall1*, and their linear transcript counterparts, have not previously been associated with pain regulation. The linear gene *Nufip1* plays a crucial role in ribophagy, which is the autophagic degradation of ribosomes (Wyant, 2018). However, the function of the circular gene is yet to be described. To gain insights into its potential role, we conducted a reactome analysis using miRWalk of the miRNAs predicted to bind to *circNufip1*. Our results suggest that *circNufip1* may be involved in pathways related to rapid depolarization, unblocking of NMDA receptors and regulation of neurexins and neurolignins. This indicates that *circNufip1* might be implicated in both peripheral and central sensitization. Some of the molecular changes in DRG from the late phase of the CAIA model are similar to what is found in models of neuropathic pain. Thus, we examined if *circNufip1* expression was altered in ipsilateral DRG from mice that underwent SNI compared to contralateral DRG and DRG from sham mice. However, we did not observe any changes in *circNufip1* or other tested targets in the mouse DRG of mice that underwent spared nerve injury (SNI) compared to contralateral and sham controls, indicating that the changes we observed in late-phase CAIA are more specific to this model. Interestingly, we found that *circNufip1* is not altered during the inflammatory phase of CAIA, suggesting that this circRNA may be involved in the residual mechanical hypersensitivity observed in the late stage of this model.

Regarding the inflammatory phase of CAIA, we have identified two circRNAs, *circVsp13* and *circMicall1,* that were upregulated in CAIA DRG. This is very intriguing as the microarray results showed that these

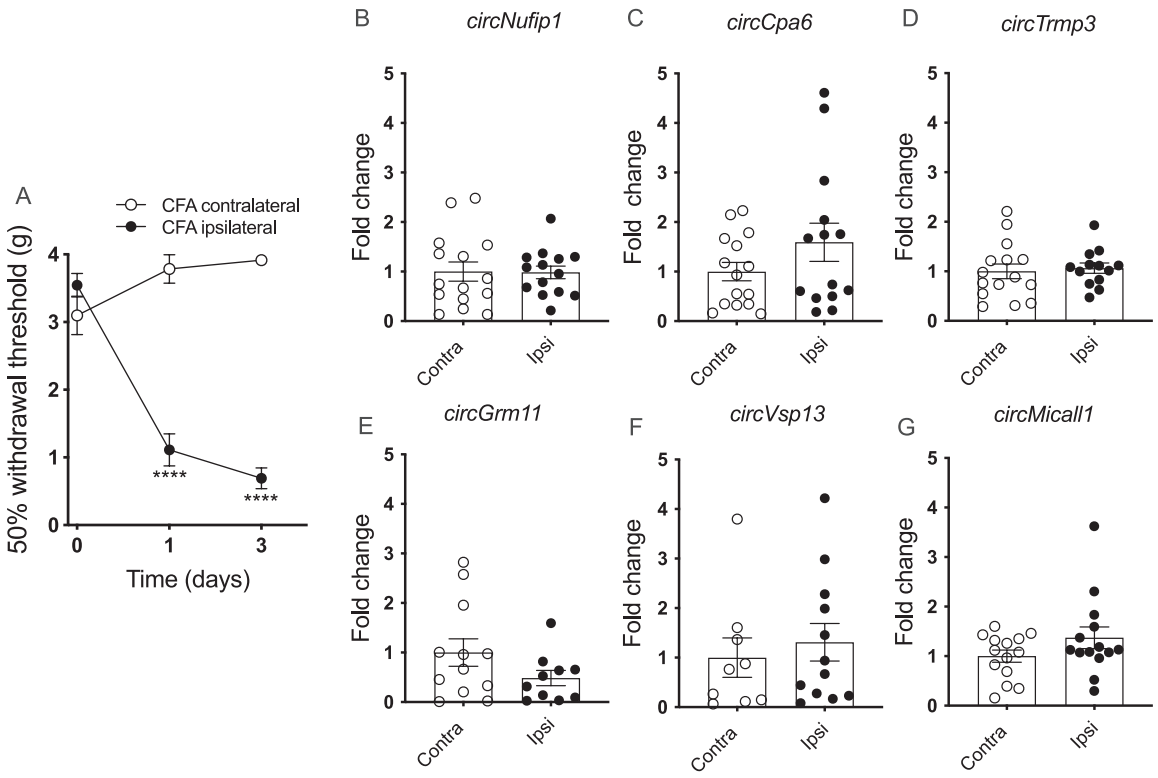

Fig. 7. Mechanical hypersensitivity and expression of selected circRNA targets from the microarray in the CFA model. (A) Withdrawal thresholds assessed by Von Frey filaments in mice with CFA-induced monoarthritis (n = 10). Two-way ANOVA was performed followed by Šídák's multiple comparisons test. Data are presented as mean +/-SEM, n = 10 mice/group. (B-G) Expression of the selected genes measured with qPCR in DRG collected 3 days after injection of CFA (n = 16, the missing data points indicate that the gene was not detected in the sample). Unpaired *t* test was preformed, and error bars represent SEM.

Table 1
Reactome analysis of the proteins that are regulated by the miRNAs predicted to bind *mmu_circRNA_27816* in *Nufip1* by the software miRWalk.

Predicted miRNA Binding Sites of mmu_circRNA_27816 in *Nufip1*
mmu-miR-7079-3p
mmu-miR-1903
mmu-miR-207
mmu-miR-7065-3p
mmu-miR-7230-5p

Name	**P-value**	**BH**
R-MMU-5673001_RAF/MAP kinase cascade	0,0053	0,7564
R-MMU-1257604_PIP3 activates AKT signaling	0,0085	0,7564
R-MMU-1660661_Sphingolipid de novo biosynthesis	0,0119	0,7564
R-MMU-6811558_PI5P, PP2A and IER3 Regulate PI3K/AKT Signaling	0,0144	0,7564
R-MMU-5576892_Phase 0 - rapid depolarisation	0,0269	0,7564
R-MMU-6794361_Neurexins and neuroligins	0,0334	0,7564
R-MMU-5673000_RAF activation	0,0334	0,7564
R-MMU-4085001_Sialic acid metabolism	0,0334	0,7564
R-MMU-383280_Nuclear Receptor transcription pathway	0,0371	0,7564
R-MMU-5654689_PI-3K cascade:FGFR1	0,0392	0,7564
R-MMU-389357_CD28 dependent PI3K/Akt signaling	0,0401	0,7564
R-MMU-438066_Unblocking of NMDA receptors, glutamate binding and activation	0,0407	0,7564
R-MMU-442660_Na+/Cl- dependent neurotransmitter transporters	0,0485	0,7564
R-MMU-5654710_PI-3K cascade:FGFR3	0,0485	0,7564
R-MMU-8853659_RET signaling	0,0491	0,7564

Table 2
Reactome analysis of the proteins that are regulated by the miRNAs predicted to bind *mmu_circRNA_44535* in *Vps13c* by the software miRWalk.

Predicted miRNA Binding Sites of mmu_circRNA_44535 in *Vps13c*
mmu-miR-107-5p
mmu-miR-129-5p
mmu-miR-7092-3p
mmu-miR-1904
mmu-miR-485-3p

Name	**P-value**	**BH**
R-MMU-1257604_PIP3 activates AKT signaling	0,0003	0,1869
R-MMU-6811558_PI5P, PP2A and IER3 Regulate PI3K/AKT Signaling	0,0012	0,3738
R-MMU-5673001_RAF/MAP kinase cascade	0,0107	0,769
R-MMU-389357_CD28 dependent PI3K/Akt signaling	0,0129	0,769
R-MMU-194840_Rho GTPase cycle	0,0223	0,769
R-MMU-4085001_Sialic acid metabolism	0,0257	0,769
R-MMU-2173796_SMAD2/SMAD3:SMAD4 heterotrimer regulates transcription	0,0289	0,769
R-MMU-1433557_Signaling by SCF-KIT	0,0317	0,769
R-MMU-212436_Generic Transcription Pathway	0,0345	0,769
R-MMU-5218920_VEGFR2 mediated vascular permeability	0,0349	0,769
R-MMU-5357786_TNFR1-induced proapoptotic signaling	0,0379	0,769
R-MMU-6794361_Neurexins and neuroligins	0,0401	0,769
R-MMU-5576894_Phase 1 - inactivation of fast Na+ channels	0,0465	0,769
R-MMU-1296041_Activation of G protein gated Potassium channels	0,0477	0,769
R-MMU-997272_Inhibition of voltage gated Ca2+ channels via Gbeta/gamma subunits	0,0477	0,769
R-MMU-114604_GPVI-mediated activation cascade	0,0485	0,769

two genes were downregulated in the late phase of CAIA, indicating that the flip in expression levels might occur during the resolution of inflammation. The linear genes *Vsp13* and *Micall1* have related

Table 3
Reactome analysis of the proteins that are regulated by the miRNAs predicted to bind *mmu_circRNA_011505* in *Micall1* by the software miRWalk.

Predicted miRNA Binding Sites of mmu_circRNA_011505 in *Micall1*
mmu-miR-7009-5p
mmu-miR-3095-3p
mmu-miR-615-5p
mmu-miR-380-3p
mmu-miR-1933-5p

Name	**P-value**	**BH**
R-MMU-8856828_Clathrin-mediated endocytosis	0.013	0.9033
R-MMU-5628897_TP53 Regulates Metabolic Genes	0.0145	0.9033
R-MMU-1257604_PIP3 activates AKT signaling	0.0259	0.9033
R-MMU-8873719_RAB geranylgeranylation	0.0341	0.9033
R-MMU-6811558_PI5P, PP2A and IER3 Regulate PI3K/AKT Signaling	0.0351	0.9033
R-MMU-212436_Generic Transcription Pathway	0.0377	0.9033
R-MMU-5673001_RAF/MAP kinase cascade	0.0454	0.9033

functions; while *Vsp13* is involved in membrane trafficking of lipids (Dziurdzik and Conibear, 2021), *Micall1* has been implicated in membrane trafficking (Frémont et al., 2017). Importantly, miRWalk analysis for *circVsp13* indicated involvement in some pathways that are shared with *circNufip1*, such as neurexins and neurolignins, but it also indicated terms related to vascular permeability and inflammation, while the miRNAs downstream of *circMicall1* imply involvement in clathrin-mediated endocytosis which is related to the function of the linear gene. The changes in inflammatory phase of CAIA were, again, specific to CAIA and not shared with CFA, another model of joint inflammation.

In addition to the top regulated genes on microarray, we also assessed the expression of 3 additional genes; *circCpa6*, *circGrm1*, *circTrpm3;* that were altered on the microarray and are encoded from the loci that were previously linked to pain regulation. While the function of these circular transcripts is unknown, they could potentially regulate the gene expression of the linear transcripts from the same loci by competing for splicing elements (Patop et al, 2019). Linear counterpart, carboxypeptidase A6 (*Cpa6*), is a metalloprotease that cleaves and regulates the levels of neurotensin, a neuropeptide which is a potent analgesic (Lyons et al., 2008; Kleczkowska and Lipkowski, 2013). Metabotropic glutamate receptor 1 (*Grm1*) was reported to regulate inflammatory pain in mice via activation of ERK pathway (Karim et al., 2001) and elevated levels of *Grm1* in spinal cord were associated with bone cancer pain in rats (Yang, 2019). Furthermore, transient receptor potential melastatin 3 (*Trpm3*), a heat-activated ion channel expressed on sensory neurons, was recently identified as a major mediator of heat hypersensitivity and spontaneous pain after chronic constriction nerve injury in mice (Wang et al., 2022) by regulating the mitochondrial calcium levels in nociceptive DRG neurons (Wang et al., 2022).

Previous studies have shown that circRNAs are highly abundant in the mouse brain, sciatic nerve and spinal cord (Rybak-Wolf, 2015; Zheng et al., 2022). In our study, we observed only mild changes in circRNA expression in the DRG microarray during late phase CAIA, with the highest fold changes observed for *circNufip1* (+1.52) and *circVps13c* (-1,49) (Table S2 and S3). With some exceptions, circRNAs are expressed at relatively low levels (Patop et al., 2019) which could potentially explain the mild fold changes detected in this study. Similarly, mild changes in circRNA levels have been reported in mouse DRG in mouse models of paclitaxel-induced neuropathic pain (Mao, 2022) and diabetic peripheral neuropathy (Zhang et al., 2020), with only a small number (15 and 16, respectively) circRNAs differentially expressed in DRG in these studies. As the backsplicing that occurs during the transcription of circRNA competes with regular splicing of linear RNA from a given gene (Patop et al., 2019), it cannot be excluded that the mild changes observed in gene expression in this study lead to more prominent changes in the mRNA produced from the identified loci. Taken together, we do not find evidence that DRG is a tissue where circRNA levels are highly regulated, and though that does not exclude a role in regulation of nociception, it renders it more challenging to investigate. However, it is important to note although microarrays have higher sensitivity for the detection of circRNA transcripts with a low abundance compared to RNA-sequencing (Li, 2019), our analysis was limited to the pre-defined set of already known 14,236 circRNA transcripts that were part of the circRNA microarray (Circular RNA Array Service. arraystar.com/circular-rna-array-service/., 2023). Thus, we cannot exclude the possibility that there might be relevant circRNAs in DRG that were not part of our assay.

This exploratory study had some limitations such as the small sample size in the microarray experiment and the lack of functional assays for the identified altered transcripts which should be further explored in future studies. Validation of the selected circRNAs from microarray by qPCR proved to be challenging. Only the DRG expression of *circNufip1*, one out of six selected circRNAs that were differentially expressed on the microarray, was subsequently validated by qPCR. Some of the reasons for discrepancies between the microarray and qPCR findings might be due to the much smaller sample size used in the microarray experiment as well as the high variability in the circRNA expression levels in DRG from the individual animals.

In conclusion, here we provide the first dataset on the circRNA landscape in the DRG from an antibody-induced arthritis model compared to DRG from a commonly used model of joint inflammation and nerve injury-indued hypersensitivity. We have identified CAIA specific expression of *circNufip1, circVps13* and *circMicall1*. These findings are relevant for advancement for our understanding of potential molecular mechanisms behind pain chronicity in RA and other painful conditions.

Funding.

This work was supported by IBSA Foundation (V.P.), Petrus and Augusta Hedlunds Foundation (V.P.), Ulla and Gustaf af Uggla Foundation (V.P.), Lars Hiertas Minne Foundation (V.P.), John J. Bonica Fellowship from International Association for the Study of Pain (V.P.) and Academy of Finland (V.P.), the European Research Council (ERC) under the European Union's Horizon 2020 research and innovation programme under the grant agreement no. 866075 (C.I.S), the European Union Seventh Framework, European Union's Horizon 2020 research and innovation programme under the Marie Skłodowska-Curie Grant Agreement number 764860 (C. I. S.), Swedish Research Council (C.I.S.), the Knut and Alice Wallenberg Foundation (C.I.S.), (C.I.S.), and by a generous donation from Leif Lundblad and family (C.I.S.).

Declaration of interests.

The authors declare that they have no known competing financial interests or personal relationships that could have appeared to influence the work reported in this paper. Zerina Kurtović reports employment with Kancera AB that is not considered to be relevant to this work.

CRediT authorship contribution statement

Zerina Kurtović: Methodology, Validation, Formal analysis, Investigation, Data curation, Writing – original draft, Visualization. **Katalin Sandor:** Methodology, Validation, Investigation, Writing – review & editing. **Freija ter Heegde:** Methodology, Investigation, Writing – review & editing. **Resti Rudijto:** Methodology, Investigation, Writing – review & editing. **Camilla I. Svensson:** Conceptualization, Methodology, Resources, Data curation, Writing – original draft, Visualization, Supervision, Project administration, Funding acquisition. **Vinko Palada:** Conceptualization, Methodology, Resources, Data curation, Writing – original draft, Visualization, Supervision, Project administration, Funding acquisition.

Declaration of Competing Interest

The authors declare that they have no known competing financial interests or personal relationships that could have appeared to influence the work reported in this paper. Zerina Kurtović reports employment with Kancera AB that is not considered to be relevant to this work.

Data availability

Data will be made available on request.

Appendix A. Supplementary data

Supplementary data to this article can be found online at https://doi.org/10.1016/j.ynpai.2023.100142.

References

Agalave, N.M., Larsson, M., Abdelmoaty, S., Su, J., Baharpoor, A., Lundbäck, P., Palmblad, K., Andersson, U., Harris, H., Svensson, C.I., 2014. Spinal HMGB1 induces TLR4-mediated long-lasting hypersensitivity and glial activation and regulates pain-like behavior in experimental arthritis. Pain 155 (9), 1802–1813.

Allen, B.L., Montague-Cardoso, K., Simeoli, R., Colas, R.A., Oggero, S., Vilar, B., McNaughton, P.A., Dalli, J., Perretti, M., Sher, E., Malcangio, M., 2020. Imbalance of proresolving lipid mediators in persistent allodynia dissociated from signs of clinical arthritis. Pain 161 (9), 2155–2166.

Bas, D.B., et al., 2012. Collagen antibody-induced arthritis evokes persistent pain with spinal glial involvement and transient prostaglandin dependency. Arthritis Rheum. 64, 3886–3896.

Cao, S., et al., 2017. Chronic constriction injury of sciatic nerve changes circular RNA expression in rat spinal dorsal horn. J. Pain Res. 10, 1687–1696.

Cao, H.-J., Huang, L., Zheng, M.-R., Zhang, T., Xu, L.-C., 2022. Characterization of circular RNAs in dorsal root ganglia after central and peripheral axon injuries. Front. Cell. Neurosci. 16, 1046050.

Chen, L.-L., et al., 2023. A guide to naming eukaryotic circular RNAs. Nat. Cell Biol. 25, 1–5.

Christianson, C.A., Corr, M., Firestein, G.S., Mobargha, A., Yaksh, T.L., Svensson, C.I., 2010. Characterization of the acute and persistent pain state present in K/BxN serum transfer arthritis. Pain 151 (2), 394–403.

Christianson, C.A., Dumlao, D.S., Stokes, J.A., Dennis, E.A., Svensson, C.I., Corr, M., Yaksh, T.L., 2011. Spinal TLR4 mediates the transition to a persistent mechanical hypersensitivity after the resolution of inflammation in serum-transferred arthritis. Pain 152 (12), 2881–2891.

Circular RNA Array Service. arraystar.com/circular-rna-array-service/. (2023).

Cohen, S.P., Vase, L., Hooten, W.M., 2021. Chronic pain: an update on burden, best practices, and new advances. Lancet 397 (10289), 2082–2097.

Descalzi, G., et al., 2015. Epigenetic mechanisms of chronic pain. Trends Neurosci. 38, 237–246.

Dweep, H., Sticht, C., Pandey, P., Gretz, N., 2011. miRWalk–database: prediction of possible miRNA binding sites by 'walking' the genes of three genomes. J. Biomed. Inform. 44, 839–847.

Dziurdzik, S.K., Conibear, E., 2021. The Vps13 Family of Lipid Transporters and Its Role at Membrane Contact Sites. Int. J. Mol. Sci. 22 (6), 2905.

Frémont, S., Romet-Lemonne, G., Houdusse, A., Echard, A., 2017. Emerging roles of MICAL family proteins - from actin oxidation to membrane trafficking during cytokinesis. J. Cell Sci. 130, 1509–1517.

Karim, F., Wang, C.C., Gereau, R.W., 2001. 4th. Metabotropic glutamate receptor subtypes 1 and 5 are activators of extracellular signal-regulated kinase signaling required for inflammatory pain in mice. *J. Neurosci.* Off. J Soc. Neurosci. 21, 3771–3779.

Kleczkowska, P., Lipkowski, A.W., 2013. Neurotensin and neurotensin receptors: characteristic, structure-activity relationship and pain modulation–a review. Eur. J. Pharmacol. 716, 54–60.

Kristensen, L.S., et al., 2019. The biogenesis, biology and characterization of circular RNAs. Nat. Rev. Genet. 20, 675–691.

Li, S., et al., 2019. Microarray is an efficient tool for circRNA profiling. Brief. Bioinform. 20, 1420–1433.

Lyons, P.J., Callaway, M.B., Fricker, L.D., 2008. Characterization of carboxypeptidase A6, an extracellular matrix peptidase. J. Biol. Chem. 283, 7054–7063.

Mao, S., et al., 2019. Circ-Spidr enhances axon regeneration after peripheral nerve injury. Cell Death Dis. 10, 787.

Mao, Q., et al., 2022. Transcriptome analysis of microRNAs, circRNAs, and mRNAs in the dorsal root ganglia of paclitaxel-induced mice with neuropathic pain. Front. Mol. Neurosci. 15, 990260.

McWilliams, D.F., Walsh, D.A., 2017. Pain mechanisms in rheumatoid arthritis. Clin. Exp. Rheumatol. 35, S94–S101.

Pan, Z., et al., 2019. MicroRNA-1224 Splicing CircularRNA-Filip1l in an Ago2-Dependent Manner Regulates Chronic Inflammatory Pain via Targeting Ubr5. J. Neurosci. Off. J. Soc. Neurosci. 39, 2125–2143.

Patop, I.L., Wüst, S., Kadener, S., 2019. Past, present, and future of circRNAs. EMBO J. 38, e100836.

Patop, I.L., Wüst, S., Kadener, S., 2019. Past, present, and future of circ RNA s. EMBO J. 38, 1–13.

Polli, A., Godderis, L., Ghosh, M., Ickmans, K., Nijs, J.o., 2020. Epigenetic and miRNA Expression Changes in People with Pain: A Systematic Review. J. pain 21 (7-8), 763–780.

Rudjito, R. *et al.* Bone innervation and vascularization regulated by osteoclasts contribute to refractive 1 pain-related behavior in the collagen antibody-induced arthritis model 2 3. *bioRxiv* 2021.04.19.440384 (2021).

Rybak-Wolf, A., et al., 2015. Circular RNAs in the Mammalian Brain Are Highly Abundant, Conserved, and Dynamically Expressed. Mol. Cell 58, 870–885.

Sohn, E.J., Park, H.T., 2020. Differential expression of circular RNAs in the proximal and distal segments of the sciatic nerve after injury. Neuroreport 31, 76–84.

Song, G.e., Yang, Z., Guo, J., Zheng, Y., Su, X., Wang, X., 2020. Interactions Among lncRNAs/circRNAs, miRNAs, and mRNAs in Neuropathic Pain. Neurotherapeutics 17 (3), 917–931.

Su, J., et al., 2015. Phenotypic changes in dorsal root ganglion and spinal cord in the collagen antibody-induced arthritis mouse model. J. Comp. Neurol. 523, 1505–1528.

Su, J., et al., 2022. Pain-like behavior in the collagen antibody-induced arthritis model is regulated by lysophosphatidic acid and activation of satellite glia cells. Brain. Behav. Immun. 101, 214–230.

Wang, J., et al., 2020. Non-coding RNAs in Rheumatoid Arthritis: From Bench to Bedside. Front. Immunol. 10, 1–9.

Wang, D., Gao, Q.i., Schaefer, I., Moerz, H., Hoheisel, U., Rohr, K., Greffrath, W., Treede, R.-D., 2022. TRPM3-mediated dynamic mitochondrial activity in nerve growth factor-induced latent sensitization of chronic low back pain. Pain 163 (11), e1115–e1128.

Wyant, G.A., et al., 2018. Nufip1 is a ribosome receptor for starvation-induced ribophagy. Science (80-.) 360, 751–758.

Xiong, W., et al., 2022. Chronic constriction injury-induced changes in circular RNA expression profiling of the dorsal root ganglion in a rat model of neuropathic pain. BMC Neurosci. 23, 64.

Yang, C., et al., 2019. SIRT1 Activation Attenuates Bone Cancer Pain by Inhibiting mGluR1/5. Cell. Mol. Neurobiol. 39, 1165–1175.

Yang, J., Cheng, M., Gu, B., Wang, J., Yan, S., Xu, D., 2020. CircRNA_09505 aggravates inflammation and joint damage in collagen-induced arthritis mice via miR-6089/AKT1/NF-κB axis. Cell Death Dis. 11 (10).

Zhang, H.-H., Zhang, Y., Wang, X., Yang, P., Zhang, B.-Y., Hu, S., Xu, G.-Y., Hu, J.i., 2020. Circular RNA profile in diabetic peripheral neuropathy: Analysis of coexpression networks of circular RNAs and mRNAs. Epigenomics 12 (10), 843–857.

Zheng, Y.-L., Guo, J.-B., Song, G.e., Yang, Z., Su, X., Chen, P.-J., Wang, X.-Q., 2022. The role of circular RNAs in neuropathic pain. Neurosci. Biobehav. Rev. 132, 968–975.

Zhou, W.Y., et al., 2020. Circular RNA: metabolism, functions and interactions with proteins. Mol. Cancer 19, 1–19.

Zhou, J., Xiong, Q., Chen, H., Yang, C., Fan, Y., 2017. Identification of the spinal expression profile of non-coding rnas involved in neuropathic pain following spared nerve injury by sequence analysis. Front. Mol. Neurosci. 10, 1–22.